Preparation, Characterization and Optimization of SnO$_2$ nano formulations to coating metallic surfaces

Geeta
Research Scholar
Baba Mastnath University, Rohtak, Haryana

PallaviBhardwaj
Associate Professor
Baba Mastnath University, Rohtak, Haryana

Dr. Sunita Devi
Assistant Professor
MKJK College, Rohtak

Sunil K. Jangra
Assistant Professor
AIJHM College, Rohtak, Haryana

Abstract

One of the major challenges in creatingextremelywell-organized nanostructure photo electrodes are to attainbettermanaging toolfor the specified morphology and enhances electrical conductivity. We create ahighly well-organized plasma-processing method to form uniform porous structures in tin as substrates. The tin oxide based Nano formulations were experimentally characterized for encapsulation potential power, particle size distribution, morphology of nanoparticles, zeta potential for stability, FTIR, and uniform entrapment. It was experimentally found that Nano formulations possessed particle size within the range of 122-290 nm and having a good encapsulation efficiency of 90-93%. These research outcomes suggested that tin oxide based nanoparticles as advance mesoporous tin oxide layering system. After performing optimizationof forming Nano composite,performed procedure of annealing, the mesoporous tin transforms into photoactive monoclinic SnO$_2$. The exceptional positive control over the Nano composite size and strong contact force created between the crystallites obtained through plasma method offers astimulatingnovel synthesis method for Nano composite resources for use in various processes like solar energy dependent water splitting.

Keywords: Tin oxide, Nano platforms, mesoporous.

Introduction

One of the fantastictasks for the recent era is to generate the accessibility of poweror energy on great demand at the terawatt level of scale[1]. In addition, various environmental concerns result in requirement for renewable energy resources to meet this ever increasing demand. Theeasy approach photo electrochemical conversion of solar or light energy into storable fuels, which is based on inexpensive and universal abundant semiconductors and catalysts, can meet these requirements[2]. Metal-oxide semiconductors are particularly appealing candidates for practical applications because of their low cost, no toxicity, abundance, and stability toward corrosion[3]. Despite intensive research efforts over the past 40 years, the efficiency of direct solar water splitting using metal oxides processed via scalable techniques still remains low[4]. One of the main bottlenecks for achieving high efficiencies with metal oxides is the mismatch between the absorption depth of visible light (up to micrometers) and the distance that the photo generated charge carriers can travel before they recombine[5].

The physical and chemical properties of nano structured materials vary significantly with size and the use of ultrafine particles evidently identifies a major technical area for materials research. Among the various nano structured materials, metal oxide nano composites have attracted increasing technological and industrial interest. Metal oxide nano composites having isolated structure consists of very small particles of a secondary phase dispersed throughout a host matrix and are of intense current significance for their physical, chemical and biological properties[6].

Specifically, geometries with a large surface-to-volume ratio, such as nanowire arrays and porous nanostructures, will decrease the distance over which charge transport has to occur and increase the amount of available surface area for catalytic reactions[7]. In this research paper, we propose a novel processing technique based on the surface treatment of tin substrates by a high flux of low-energy helium ions[8]. This provides an efficient route for the formation of porous metallic nanostructures that, after oxidation, can be used as photo anodes for solar water splitting.

Materials and Methods

Materials

$SnCl_4.5H_2O$ and NH_4OH were procured from Hi-Media Pvt. Ltd. Mumbai (India). All chemicals used in the present research were of analytical reagent grade. All yields refer to isolated products after purification. Polycrystalline tin discs (30 mm in diameter and 0.5 mm in thickness) were cut from a rod of rolled tin and mechanically polished to a mirror finish. After polishing, they were rinsed in methanol and acetone and no further treatment was applied.

Preparation of SnO$_2$ nanoparticles

$SnCl_4.5H_2O$ (0.5gm) was added to 100 ml of distilled water followed by the drop wise addition of NH_4OH (0.5M) with magnetic stirring for 8 h. The dropping rate must be well controlled for chemical homogeneity. The resulting precipitate was washed with distilled water and dried at $120°C$ for 20 h. The dried powder was further calcined at $410°C$ in air for 1 h resulting in the formation of SnO_2 nanoparticles[9].

Preparation of SnO$_2$ nanoparticles

0.5gm of $SnCl_4.5H_2O$ was dissolved in 100 ml of distilled water

↓

Dropwise addition of NH_4OH (0.5M) with magnetic stirring till precipitate formed

↓

Precipitate was washed with distilled water and dried at $120°C$ for 20 h to form dried powder

↓

Dried powder was further calcined at $410°C$ in air for 1 h resulting in the formation of SnO_2 nanoparticles

Experimental design

The optimization of SnO_2 nanoparticles were experimentally analyzed by Central composite design expert software. As per the standard procedure, the assorted design was engaged in response surface curve results. Two factorial designs were favored for optimization of nanoparticles. This design was formulated to achieve the smallest size of particles and maximum encapsulation efficiency. All additional variables were equivalently set aside. 13 trial runs conceded out are depicted in Table 1. Experimental datawere analyzed statistically[10].

Characterization of SnO_2 nanoparticles

Zetasizer Nano ZS-90 was engaged to figure the mean size range of nanoparticles and their exact size distribution[11,12].The unbound SnO_2 quantity in the supernatant experimentally generated after sky-scraping speed 8900 rpm centrifugation at 4˚C for 38 minutes was analyzed by an instrument UV spectrophotometer[13]after that% encapsulation efficiency was mathematically evaluated using following formula:

Percentage % Entrapment efficiency of Nano formulation = (Total Drug-Unbound Drug/Total Drug) × 100

The surface morphology of SnO_2 nanoparticles were analyzed by an instrument name TEM(transmission electron microscope). The Nano formulations were loaded on a Cu grid and above 65,000 magnification factors and 75,000V accelerating EMF was occupied to arrest the TEM image[14].SEM produces very high-resolution scan of each Nano formulations having particle in the ange of 10 nm[15]. Atomic force microscopy (AFM) has very-large-resolution power of microscopy, with high resolution power, around 1200 times superior than the optical diffraction method[16]. FTIR[17] analysis of SnO_2 nanoparticles was analyzed by Fourier transform infrared spectrophotometer in range of wave number 4500–500 cm^{-1}.

Results and Discussion

Optimization of the formulation variable

All through experimentally outcomes revealed that both, $SnCl_4.5H_2O$ and NH_4OHinfluenced the particle size as well as encapsulation efficiency of nanoformulations[9]. To calculate the effectiveness of $SnCl_4.5H_2O$ and NH_4OH on the particle size (X1) and encapsulation efficiency (X2) their concentrations were varied between two levels i.e. maxima & minima. The results

were then statistically analyzed[10]. The response-encapsulation efficiency (X2), response-particle size (X1) is fitted best in the reduced quadratic model after normal logarithmic conversion of data.The effect of A and B (independent variable) on size and fraction (variable) is represented by the sign and number/size of effect coefficients, first order kinetics, interaction terms, and second order kinetics.

The optimized batch of SnO_2 nanoparticles were found to have the particle size of 128 nm (Fig 1) having zeta potential value of -45.1 mV (Fig 2) with minimum particle size range (122-290 nm) and with greatest entrapment efficiency (90-93%) (Fig, 3,4) was found from design expert software data Table 1. Increase in NH_4OH concentration enhances entrapment efficiency to greater extent. As we find at low concentration of $SnCl_4.5H_2O$ and NH_4OH, the encapsulation efficiency was less[9].

Particle size and Zeta potential

NPs were analyzed for size and zeta (stability) potential measurements by dynamic light scattering. The optimized nanoparticles size was found to have 240.8 nm (Fig 1). SnO_2nanoformulations have a zeta potential of -45.9 mV (Fig 2), signifying Nano formulation stability[18].

Percentage encapsulation efficiency

The encapsulation efficiency depends upon the nature of the method employed, the extent polarity of the molecule, the molecular nature of encapsulating materials and media for the synthesis of nanoparticles[19]. The percentage of encapsulation efficiency was 90-93 % respectively for SnO_2nanoformulations.

Morphological characterization of SnO_2nanoformulations by TEM, SEM and AFM

The size of particle, their shape and particle dimension of nanoparticles significantly influence drug release rate, their solubility kinetics and dissolution process of a molecule/drug. Migration of nanoparticles to a variety of body partsis according to their shape of nanoparticles, their size and dimension of particles. The SnO_2nanoformulations were experimentally originateas segregated, spherical in shape having particle of 24 - 45 nm size range (Fig 3 SEM image analysis established that the nanoformulations have spherical in morphology (Fig 4). AFM offers

high resolution representing the intensity of the color reflects the altitude of the particle. A various range of particle sizes can be identified, from 2 nm to 3 mm (Fig 5). AFM takes concerning 1/4 of the time to get data as compare with SEM/TEM.

DSC Analysis

The DSC thermo gram of SnO_2 nanoformulations displays two endothermic peaks[20]. First endothermic progress crests at 272˚C, which is of low intensity. The high-intensity peak is sharp, that affirmed crystalline nature of the molecule. It was investigated that all crests in DSC diagram were not sharp, which confirmed that nanoformulation is amorphous and nanoformulations drug was ideal in its amorphous nature. The DSC thermo gram of SnO_2 nanoformulations loaded on metallic surface comes to be show endothermic peak crests at almost 398˚C, which is of low power and alludes to the softening nature of SnO_2 and disintegration begins after 419˚C. The peak hump is of low power and isn't sharp, that affirmed crystalline or uniform arrangement of metal on the surface of metal. The peak is of low force and isn't sharp, that affirmed indistinct nature (Fig 6).

FTIR Analysis of Drug Samples

The FTIR spectroscopy was used to infer SnO_2 nanoformulations interaction with NH_4OH as well as to confirm the formation of nanoformulations. FTIR spectrum of SnO_2 shows absorption bands at 2814 cm^{-1} showing stretching bond for the terminal –SO groups (Fig 7). FTIR spectrum 1021 cm^{-1} in SnO_2 due to the formation of weak intermolecular bonds such as dipole-dipole interaction, and weak Van der Waals (depends upon molecular mass). SnO_2 and NH_4OH reveal characteristic peaks in FTIR spectrum. Although peak intensity was decreased, bands were not shifted, signifying there is no chemical bond among SnO_2 and NH_4OH. Figure 9C represented the FTIR spectrum of the physical combination of SnO_2 and NH_4OH.

Nanoparticles loaded on surface of metallic surface

After actionof low-energy He^+, the tin surfaces display a nanoformulations surface morphology consisting of nanometric filaments with an open interconnected structure. The type of morphology observed at 1500°Ctemperature. The formation process of this structures has been evaluated in detail and appears to be related to the synthesis and coalescence of helium bubbles

in the near-surface region, leads tosurface swelling. At 1500 °C, the nano size filaments have a range of 100−200 nmdiameter. We recently discovered that these filaments have a internal crystallinestructure[21]. Such nanostructures are formed when the flow of particles to the surface is high enough. The image on the right shows a high-intensity helium beam interacting with a tin surface. With a porosity of up to 90%, nanostructured tin absorbs 94% to 97% of the light in the visible range, while polished targets reflect more than 50% of the light. Indeed, nanostructures have up to 90% porosity on the surface and up to 50% porosity near the base. The specific surface area of the metal tin oxide film can be about 20 times higher than the geometric surface area measured by nitrogen adsorption (BET).

CONCLUSIONS

Nanotechnology development creates a new efficient technique to create highly efficient electronic equipments. Various nanoformulations are market these days to raise the electrical conductivity of various semiconductors. We investigate both qualitatively and quantitatively evolution of SnO_2 nanoformulations. In this research paper, we have proposed a novel plasma-assisted processing technique to makeuniform surface nanostructures on metals surface to raise the conductive efficiency. This top-down loom guarantees superior connectionof different crystallites toavoid electrical conductivity hindrances. The optimized 13 steps leads to make annealing procedure that minimizes the concentration of defects, the mesoporous metallic tin transforms into nano structured monoclinic SnO_2. The excellent control over the feature size with the helium-plasma technique along with its effectiveness with a broad range of metals offers an exciting new synthesis route for nanostructured materials for use in processes such as solar water splitting.

Table 1: Effect of concentration ofSnCl₄.5H₂O andNH4OH gm on Particle size and entrapment efficiency.

Experimental Run	Factor 1 A SnCl$_4$.5H$_2$O	Factor 2 B NH$_4$OH M	Response 1 Particle size nm	Response 2 Entrapment efficiency %
1	0.50	0.50	238.63	92.40
2	0.60	0.55	128.98	93.02
3	0.40	0.60	178.20	92.64
4	0.30	0.65	278.10	90.16

5	0.35	0.70	207.90	91.01
6	0.25	0.40	148.28	93.00
7	0.55	0.30	288.20	91.93
8	0.50	0.40	121.18	93.00
9	0.60	0.50	228.18	93.03
10	0.45	0.55	292.80	92.24
11	0.35	0.50	209.60	91.92
12	0.40	0.65	299.28	92.63
13	0.45	0.40	209.60	91.04

Table 2: Statistical parameters of Response surface model

Response factor	Modal								Lack of fit	
	F value	Prob, > F	R^2	Adjs. R^2	Pred. R^2	Adq. Prec.	C.V	Std. Dev.	F value	Prob. > F
Y1	21.37	0.94	0.5938	0.2442	0.6121	4.578	10.42	16.38	3.16	0.5322
Y2	48.11	0.40	0.1411	0.1574	0.6534	2.221	5.78	2.72	0.21	0.9010

Figure 1. PSA image of SnO$_2$nanoparticles
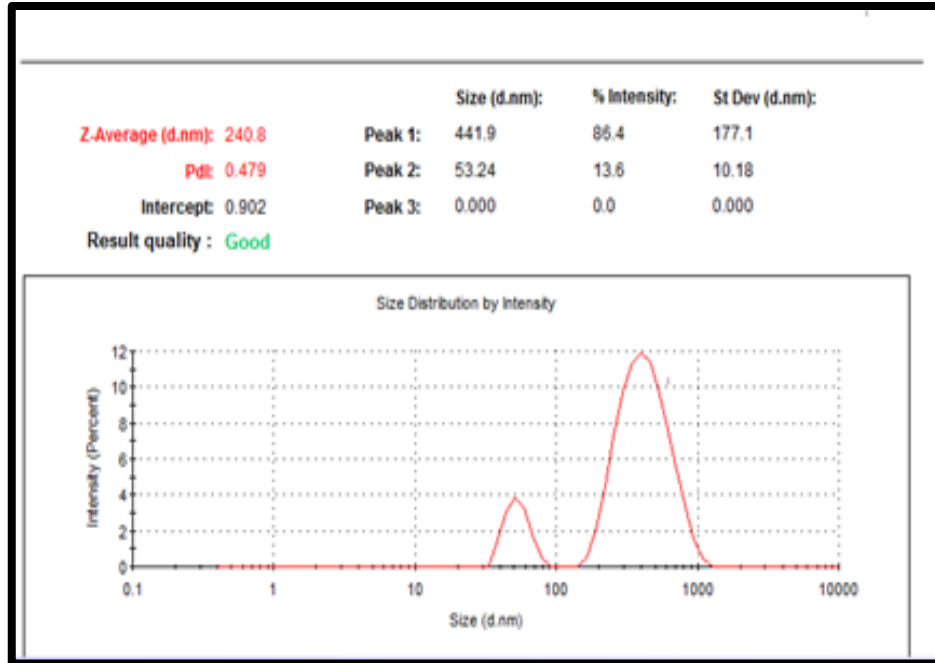
Figure 2. Zeta potential of SnO₂nanoparticles
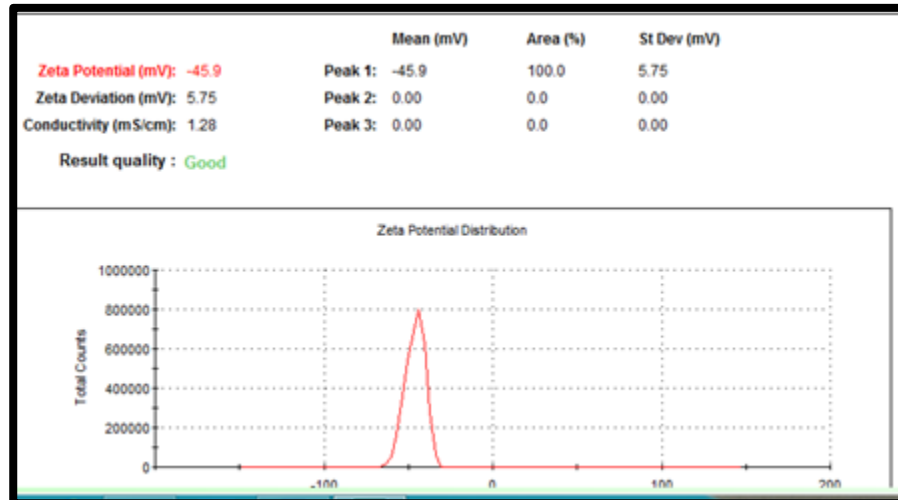
Figure 3: TEM image of SnO₂nanoparticles
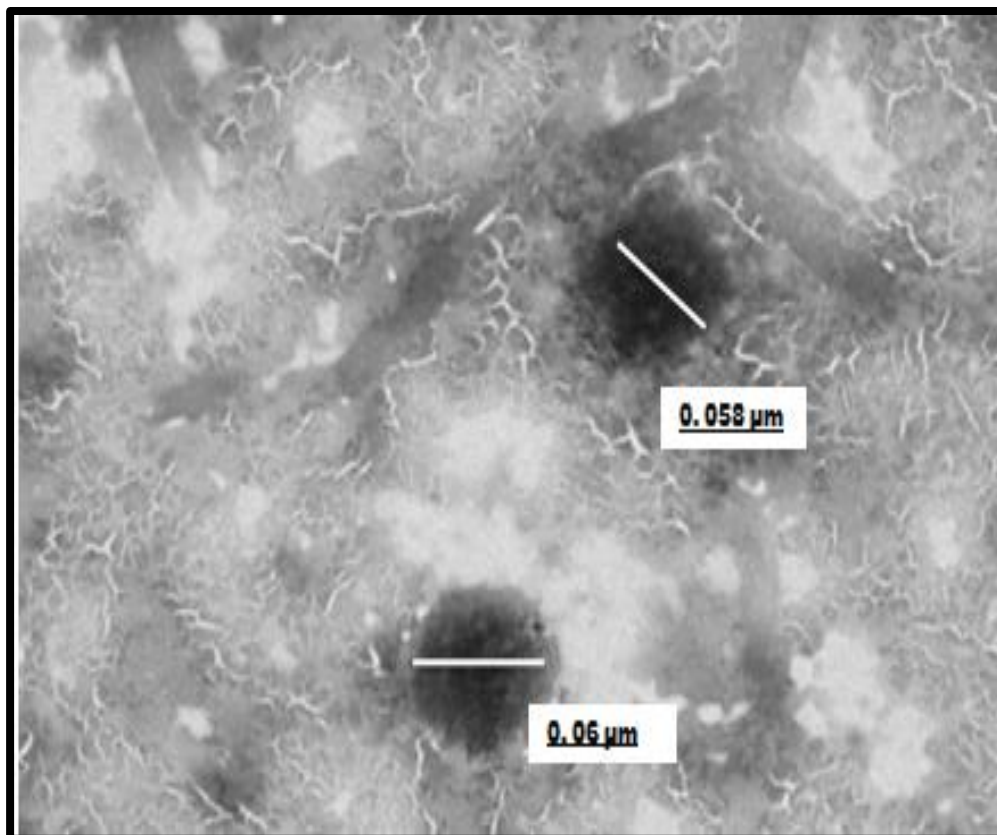
Figure 4: SEM image of SnO$_2$nanoparticles
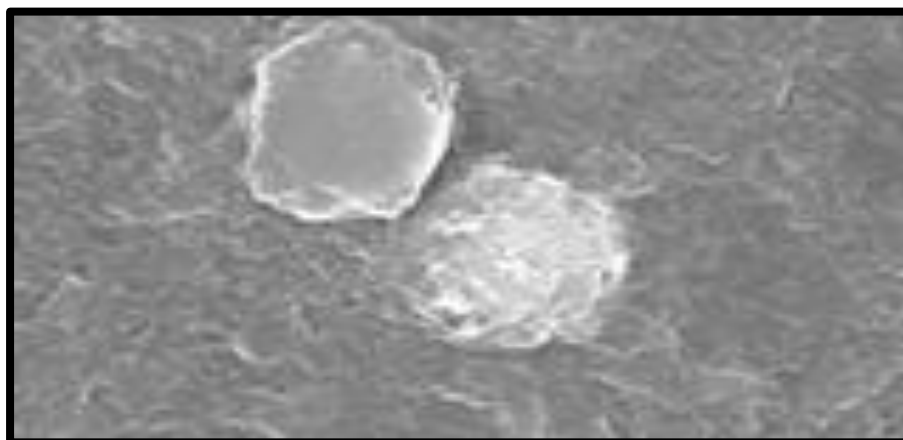
Figure 5: AFM image of SnO$_2$nanoparticles
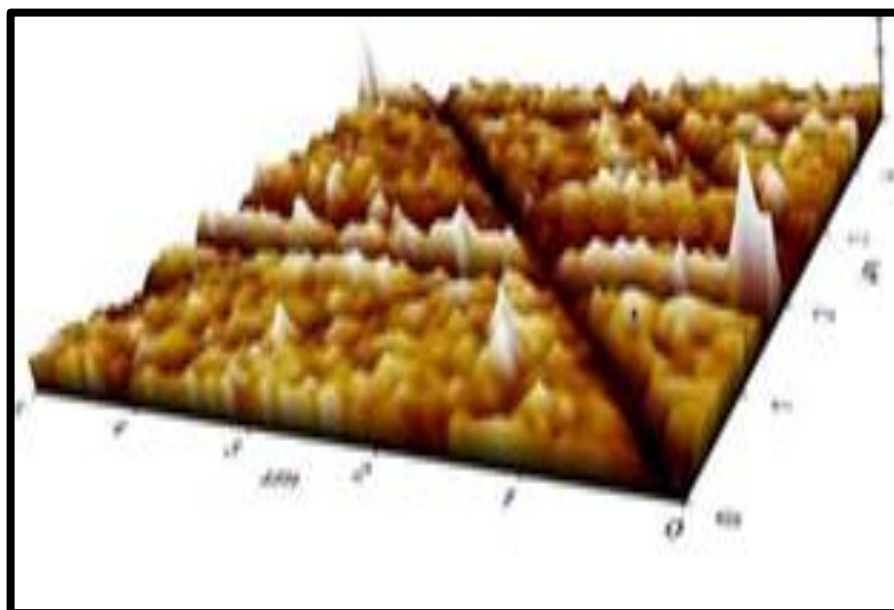
Figure 6. DSC of SnO$_2$nanoparticles
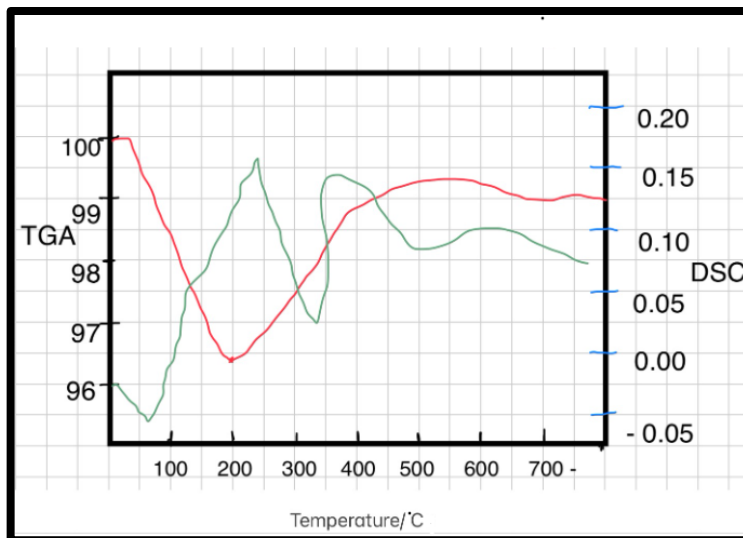
Figure 7: FTIRspectra of (A)SnO$_2$(B)SnO$_2$nanoparticles
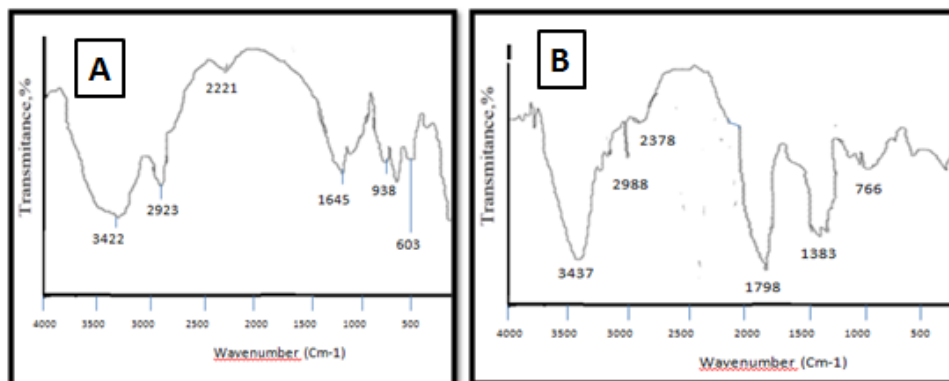
References

1. Haegel, N. M., Atwater Jr, H., Barnes, T., Breyer, C., Burrell, A., Chiang, Y. M.,.&Bett, A. W. (2019). Terawatt-scale photovoltaics: Transform global energy. *Science*, *364*(6443), 836-838.

2. Ezugwu, C. I., Liu, S., Li, C., Zhuiykov, S., Roy, S., &Verpoort, F. (2022). Engineering metal-organic frameworks for efficient photocatalytic conversion of CO2 into solar fuels. *Coordination Chemistry Reviews*, *450*, 214245.

3. Prabhakar, R. R., Septina, W., Siol, S., Moehl, T., Wick-Joliat, R., & Tilley, S. D. (2017). Photocorrosion-resistant Sb 2 Se 3 photocathodes with earth abundant MoS x hydrogen evolution catalyst. *Journal of Materials Chemistry A*, *5*(44), 23139-23145.

4. Abanades, S. (2019). Metal oxides applied to thermochemical water-splitting for hydrogen production using concentrated solar energy. *ChemEngineering*, *3*(3), 63.

5. Lu, N., Jing, X., Zhang, J., Zhang, P., Qiao, Q., & Zhang, Z. (2022). Photo-assisted self-assembly synthesis of all 2D-layered heterojunctionphotocatalysts with long-range spatial separation of charge-carriers toward photocatalytic redox reactions. *Chemical Engineering Journal*, *431*, 134001.

6. Pourrahimi, A. M., Olsson, R. T., &Hedenqvist, M. S. (2018). The role of interfaces in polyethylene/metal-oxide nanocomposites for ultrahigh-voltage insulating materials. *Advanced Materials*, *30*(4), 1703624.

7. Zhang, X., Li, D., Bourgeois, L., Wang, H., &Webley, P. A. (2009). Direct electrodeposition of porous gold nanowire arrays for biosensing applications. *ChemPhysChem*, *10*(2), 436-441.

8. Ikramova, S. B., Utegulov, Z. N., Dikhanbayev, K. K., Gaipov, A. E., Nemkayeva, R. R., Yakunin, V. G., ... & Timoshenko, V. Y. (2022). Surface-Enhanced Raman Scattering from Dye Molecules in Silicon Nanowire Structures Decorated by Gold Nanoparticles. *International journal of molecular sciences*, *23*(5), 2590.

9. Katti, K. V. (2005). Synthesis and reactivity in inorganic, metal-organic and nano-metal chemistry. *Synthesis and Reactivity in Inorganic, Metal-Organic, and Nano-Metal Chemistry*, *35*(1), 1-2.

10. Sethi, N., Bhardwaj, P., Kumar, S., &Dilbaghi, N. (2019). Development and Evaluation of Ursolic Acid Co-Delivered Tamoxifen Loaded Dammar Gum Nanoparticles to Combat Cancer. *Advanced Science, Engineering and Medicine*, *11*(11), 1115-1124.

11. Vivek, V., Sethi, N., &Kaura, S. (2022). Green synthesis and evaluation of antibacterial activity of zinc nanoparticles from Calotropisprocera leaves.

12. Suman, J., Neeraj, S., Rahul, J., &Sushila, K. (2014). Microbial synthesis of silver nanoparticles by Actinotalea sp. MTCC 10637. *American Journal of Phytomedicine and Clinical Therapeutics*, *2*, 1016-23.

13. Shi, Z., Chow, C. W., Fabris, R., Liu, J., & Jin, B. (2022). Applications of online UV-Vis spectrophotometer for drinking water quality monitoring and process control: a review. *Sensors*, *22*(8), 2987.

14. Egerton, R. F. (2008). Electron energy-loss spectroscopy in the TEM. *Reports on Progress in Physics*, *72*(1), 016502.

15. Carlson, B. D., & Donavan, D. T. (2008). SEM. *Sport Marketing Quarterly*, *17*, 154-62.

16. Giessibl, F. J. (2003). Advances in atomic force microscopy. *Reviews of modern physics*, *75*(3), 949.

17. Berger, F., Beche, E., Berjoan, R., Klein, D., &Chambaudet, A. (1996). An XPS and FTIR study of SO2 adsorption on SnO2 surfaces. *Applied surface science*, *93*(1), 9-16.

18. Marsalek, R. (2014). Particle size and zeta potential of ZnO. *APCBEE procedia*, *9*, 13-17.

19. Jyothi, N. V. N., Prasanna, P. M., Sakarkar, S. N., Prabha, K. S., Ramaiah, P. S., &Srawan, G. Y. (2010). Microencapsulation techniques, factors influencing encapsulation efficiency. *Journal of microencapsulation*, *27*(3), 187-197.

20. Ungureanu, A. M., Jitaru, I., &Gosnea, F. (2013). Mn doped SnO2 prepared by a sol-gel method. *UPB Sci Bull Ser B Chem Mater Sci*, *75*, 43-52.